Fracture Mechanics of Concrete and Concrete Structures -
High Performance, Fiber Reinforced Concrete, Special Loadings and Structural Applications- B. H. Oh, et al. (eds)
ⓒ 2010 Korea Concrete Institute, ISBN 978-89-5708-182-2

# Double-edge wedge splitting test: preliminary results

M. di Prisco, M.G.L. Lamperti & S. Lapolla
*Department of Structural Engineering, Politecnico di Milano, Italy*

ABSTRACT: A new technique to identify the residual strength in the post-cracking regime has been developed at the Politecnico di Milano for thin-walled Fibre Cementitious Composite structures. The idea is that to spatially uncouple compressive stresses from tensile stresses in an indirect tensile test, close to Brazilian test, by introducing only a mode I crack opening. The uncoupling caused by a double notch allows the test procedure to identify the real toughness associated to fibre pull-out. The identification of in plane strength vs. crack opening for shear and diffusion stress states, especially for oriented cast flows favoured by self compacting mixes, suggests the use of this new technique that can be also easily coupled to bending tests. In this paper the main experimental details will be discussed, while in a companion paper the reliability of the identification procedure with reference to bending tests on self compacting fiber reinforced concrete for different casting procedures is investigated.

## 1 INTRODUCTION

High Performance Fiber Reinforced Cementitious Composites (HPFRCC) are quite complex materials which need an orthotropic description both in uniaxial tension and in uniaxial compression. Due to the alignment of fibers caused by the casting flow made possible by their self compacting performance, they often show a small scatter in the tensile response when the casting flow is well oriented or a large scattering when a random casting flow procedure is carried out that causing a random fiber distribution in the average plane. Often fiber dispersion highlights even a significant variation in the small thickness, and therefore it is necessary to take into account this characteristic when a bending behavior is required, but this information does not affect shear and membrane behaviors, which are affected only by average characteristics in the thickness. The principal aim of the new test is to reproduce the stress distribution on the sections of a notched specimen loaded in pure tension, without any crosswise compressive stresses, contrarily to what occurs in Bending and Brazilian tests, where compressive and tensile stresses act on the bending/splitting plane. Following the analogy between Three Point Bending and Wedge Splitting Test, suggested by Brühwiler e Wittmann (1990), a Double-Edge Wedge Splitting Test (DEWST) is here proposed (Fig. 1) also to simplify the loading device commonly used in direct tension test.

To obtain a very compact test set-up, the cylinder and the outer wedge, typical of the WST, are substituted by two opposite wedge-shaped notches. On the notch lips suitably treated steel plates are applied to guarantee low sliding friction with two steel load cylinders. The obtained set-up reproduces also, without cylindrical symmetry, a sort of Double Punch Test proposed by Chen & Yuan (1980, Fig. 2).

A possible advantage of the DEWST, shared with traditional splitting tests on cylinders, is the possibility of carrying out tensile tests by applying compressive loads, thus avoiding the typical complications of the direct application of a tensile load on the specimen (like gluing specimen's extremities to the press platens, or providing the specimen with particular load-transferring devices). Moreover, the absence of highly-localized compression stresses is a plus in the case of ductile materials, where the small loaded area may undergo significant plastic deformations. Therefore it can be regarded as an extension of Brazilian and Wedge Splitting Tests. These aspects, joined to the need of doing tests also on compact-samples extracted from full-size structures, has addressed the choice towards indirect tensile methods. Although the evolution of test methods inherited from Fracture Mechanics of Concrete have suggested to International Standards the employment of bending tests for their executive simplicity and for the confidence provided by an extensive and time-spread experimental application, the coupling of an unnotched four point bending test with two tests like that presented, considering two notched planes at right angles in the two extremities and subsequently four small rectangular prisms sawn by the four pieces obtained after carrying out the two DEWS tests discarding the cracked zones, could really give the designer all the information strictly necessary for a careful design procedure.

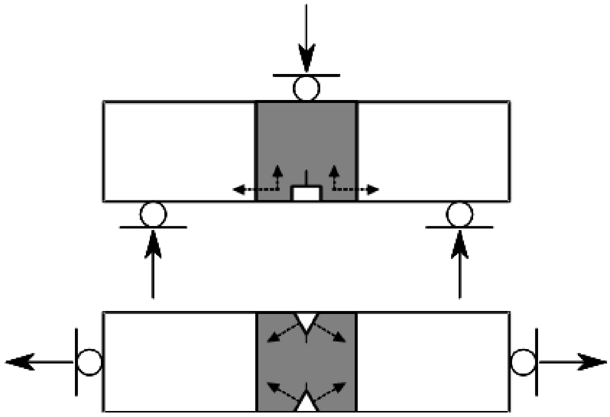

Figure 1. Wedge Splitting as a “compact” Third Point Bending Beam (Brühwiler and Wittman 1990) and Double Sided Wedge Splitting as a Direct Tension Specimen .

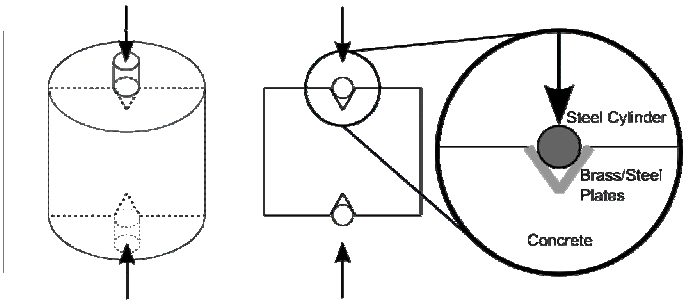


Figure 2. (a) Double Sided Wedge Splitting as section of Double Punch Test.

## 2 THE TESTING TECHNIQUE

The particular arrangement used to apply the compressive load, namely two steel cylinders acting on 45°-shaped notches provided with steel/brass plates, makes sure that two compressive stress arches are established between the loading punches. In this way, the mid-span section is subjected to uniaxial tensile stresses and the measured strength will be very close to what measured in a uniaxial tension test where the elastic zone, which is the main source of energy release in the crack propagation process, is very reduced. The two notches prevents the simultaneous presence of compressive stresses oriented along the vertical direction as occurs in Brazilian test (= biaxial stress state): this stress pattern disturbs fiber pull-out as observed in splitting tests, because it could increase bond strength.

The friction between the cylinder and the metal surfaces reduces the effective load applied to the sample and introduces a tangential component applied to the sliding surface. Different metal couplings and various lubricants were compared to evaluate the friction reduction between the cylinders and the metal sliding surfaces. Starting from literature friction coefficients, three different solutions were considered: steel and brass in direct contact, PTFE layer insertion and use of graphite as lubricant. A particular test device aimed to simulate the behavior of the specimen subjected to vertical load by measuring the tensile force really transmitted to the fracture surface was get ready. At the end, the best solution was reached with a ratio between measured load on fracture and applied load close to 89% by using graphite as lubricant.

## 3 SET-UP AND EXPERIMENTAL PROGRAMME

An electromechanical INSTRON press with a maximum load capacity of 100 kN was used. The tests were displacement-controlled by imposing a constant stroke rate (0.2÷0.5 μm/s) to the loading machine, via the displacement transducer of the press. Each side of the specimens (Front and Rear) was instrumented by three displacement transducers (LVDT), at the tip of the upper and lower notch and in the middle of the tiles (Fig. 3). The specimen geometry is described in Table 1: the critical depth and the cylinder diameter are respectively 80 and 10 mm for the whole test set. The load detail is clearly shown in Figure 3: the upper press platen was free to rotate with respect to the load axis.

Table 1. Types and geometry of investigated specimens.

| Specimen Length | Type depth | Side diameter | Critical | Cylinder |
|---|---|---|---|---|
| | | mm | mm | mm |
| P7 | A | 100 | 80 | 10 |
| P8 | A | 100 | 80 | 10 |
| P9 | A | 100 | 80 | 10 |
| P1-120 | B | 120 | 80 | 10 |
| P4-120 | B | 120 | 80 | 10 |
| P7-120 | B | 120 | 80 | 10 |

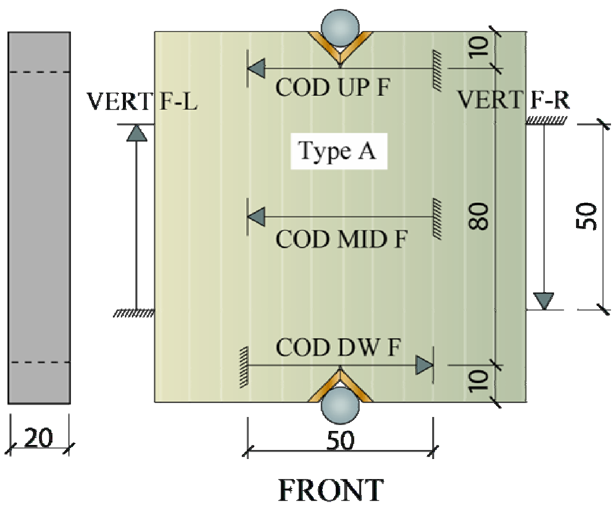


(a)

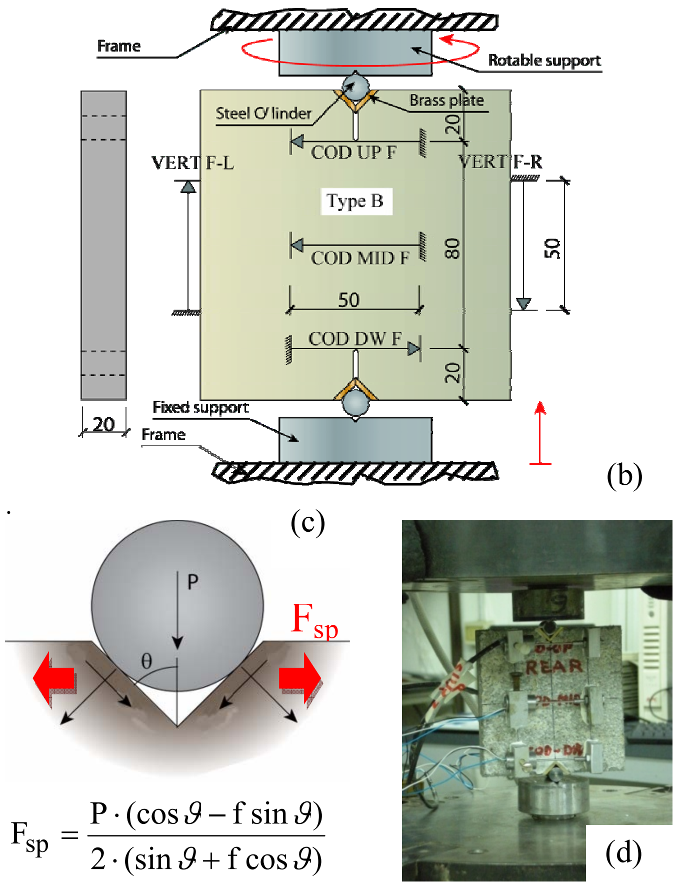


$$F_{sp} = \frac{P \cdot (\cos \vartheta - f \sin \vartheta)}{2 \cdot (\sin \vartheta + f \cos \vartheta)}$$

f friction coefficient

Figure 3. Experimental test set-up;(a) type A; (b) type B; (c) load details; (d) test set-up view.

## 4 TEST RESULTS

### 4.1 *Material properties*

The composite (Table 2) was selected by comparing different solutions starting from the aggregates generally used by the precast producer and limiting their maximum size to 2 mm (di Prisco et al. 2008). Preliminary tests on shrinkage allowed us to estimate the quite large strain that was expected due to the significantly large fraction of fine aggregates used in the mix. An average cubic compressive strength of 143 MPa and an elastic modulus close to 40 GPa characterized the material in the preliminary qualification. No specific procedure was used in the casting process to orient steel fibers and this technological detail can be regarded as the main reason of the huge scattering (Ferrara et al. 2010). Double Edge Wedge Splitting specimens were extracted by an original plate, 20 mm thick, used to prepare twelve unnotched plates tested in bending. It is obvious that any accumulation of steel fibers in the bottom part of the thin specimens can affect bending tests, but scantly the average force in DEWS test: anyway such occurrence can cause a rotation along the vertical axis of the mean plane at right angle with the crack opening direction. In order to better explain the experimental results obtained by means of the two geometries discussed (Type A and B, Fig. 3), an example of both specimens are discussed in the following paragraphs.

Table 2. Mix design.

| | Content<br>kg/m$^3$ |
|---|---|
| Cement type I 52.5 | 600 |
| Slag | 500 |
| Water | 1200 |
| Superplasticizer | 33 (l/m$^3$) |
| Sand 0-2 mm | 983 |
| Fibres ($l_f$=13mm; $d_f$=0.16mm) | 100 |

Table 3. Geometry and mechanical properties of investigated specimens.

| Specimen | Thickness | Peak load | $f_{t,max}$ | $f_{t,m}$ | Main opening |
|---|---|---|---|---|---|
| | mm | kN | MPa | MPa | |
| P7 | 23 | 7.56 | 3.65 | | down |
| P8 | 22 | 13.87 | 6.71 | | up |
| P9 | 21 | 19.97 | 9.12 | 6.78 | up |
| P1-120 | 21 | 16.19 | 7.83 | (st.dev. | down |
| P4-120 | 21 | 10.66 | 5.16 | ±2.05) | down |
| P7-120 | 22 | 16.98 | 8.21 | | down |

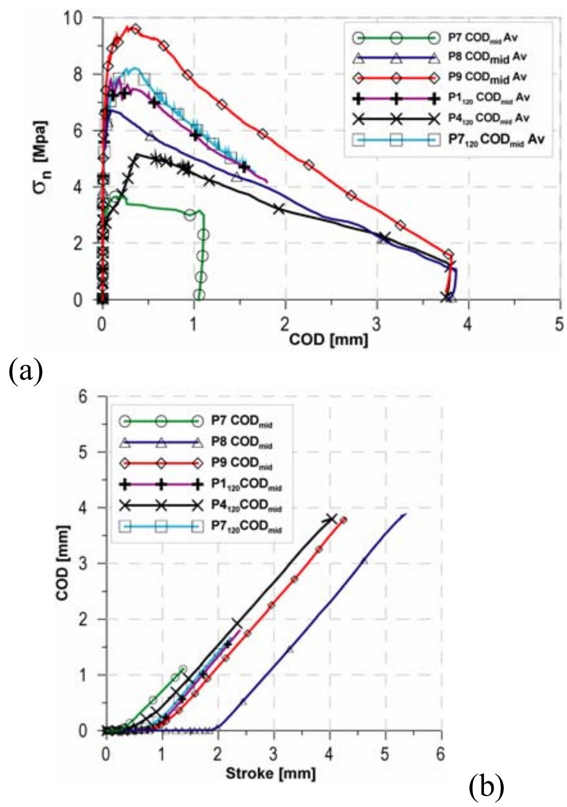


Figure 4. Overall specimen tests: (a) Nominal stress vs. COD curve; (b) COD vs. stroke curves.

The response of the whole test set is shown in Figure 4 in relation to nominal stress $\sigma_N$ vs. COD. A large scattering can be observed in DEWS tests (Fig. 4). In the stable crack propagation stroke is the most sensible displacement parameter, while in the pull-out phase stroke and average COD growth are comparable (Fig. 4b).

### 4.2 *Double-edge wedge splitting tests*

The main results related to the first geometry (Type A) are shown in Figure 5. First of all the main parameters used to control the test are described (Fig. 5a): it is evident how stroke monotonically increases along the overall loading test steps and therefore it can be adopted as feedback parameter. The load highlights a first "knee" due to steel cylinder vertical displacement settlement. The crack propagation is not symmetric as expected (Fig. 5b) and starts in this case from the upper fiber. It is interesting to underline that there is not any reason for which top or bottom process zone could prevail: the only reason should be related to fiber distribution, and also the difference between the crack opening measured along the critical depth region can be assumed as a measure of the homogeneity of steel fibers inside the specimen volume. The specific measure of crack opening along the mid, up and bottom LVDT gauges are respectively shown in Figures 5c,d,e with reference to both the front and rear sides: a significant comparison between the mean values recorded on the two sides is also shown (Fig. 5f).

Finally the rotations along the two axes, that at right angle with the tile average plane and the vertical axis of the average plane at up, mid and bottom LVDT gauges locations are computed according to the following equations (Figs 5g,h):

$$\varphi_{mid-down} = \frac{COD_{down} - COD_{mid}}{d_{mid-down}} \quad [1]$$

$$\varphi_{up-down} = \frac{COD_{down} - COD_{up}}{d_{up-down}} \quad [2]$$

where $\varphi_{\text{mid-down}}$ and $\varphi_{\text{up-down}}$ are the relative distances measured between the gauge axes. In the specimen P9 the in plane rotation is about three times larger than the out of plane one at the test end, but, while the former grows in the unstable crack propagation, the latter grows in the stable propagation.

At the peak load the former is less than one sixth the latter. This means that the in plane rotation during the pull-out phase is affected by fibers distribution on the critical depth, while the stable crack propagation is more affected by matrix, whose strength is much more homogeneous, and by fiber dispersion in the thickness which is small.

The good superposition of the curves for both rotations confirms the plane cross section assumption during crack propagation in the matrix as well as in the pull-out phase. The last observation for P9 specimen test concerns the crack opening measured by the bottom transducer on the rear side: although the set-up should cause always a positive crack opening, due to the out of plane rotation, the LVDT measure is weakly negative (Fig. 5e). Similar considerations can be argued for specimen type B (Fig. 6), with the only exception that the out of plane rotation is so large that all the LVDT measures on the front side are negative and the crack propagates from bottom fiber to the top one.

## 5 NUMERICAL SIMULATION

The type B specimen was also numerically investigated to highlight the stress pattern inside the specimen when a homogeneous mono-phase constitutive behavior is assumed for HPFRCC material. For uniaxial tension, Hordijk's constitutive law (Hordjik, 1991) was adopted in the numerical modeling of tension softening, instead of a bilinear softening law (di Prisco et al. 2004, 2009), because this guarantees a mesh independent result in the Finite Element code used (DIANA, Release 9.3) due to an automatic choice of the characteristic length set on the basis of finite element size (Bazant & Cedolin, 80).

The post-peak dissipated energy measured in the DEWS test carried out was used for the identification procedure of the softening parameters, while in uniaxial compression only compressive strength was adopted. The mesh adopted is quite regular (Fig. 7); the numerical test is displacement controlled by assuming a negligible friction and fixed contact lines between the steel cylinder and the inclined steel plates. The pinned connections are monotonically moved along the normal direction with respect to the contact steel plates and were free to slide along the 45° inclined plane parallel to the notch lips. The vertical load is determined on the basis of the reactions suitably projected along the critical axis that connects the tip notches. A total strain fixed crack approach was selected. The solution investigated is forced to be symmetric due to the lack of any defect and the perfect homogeneity assumption for the material adopted: only scantly geometrical defects due to a not perfect symmetry of the mesh are considered.

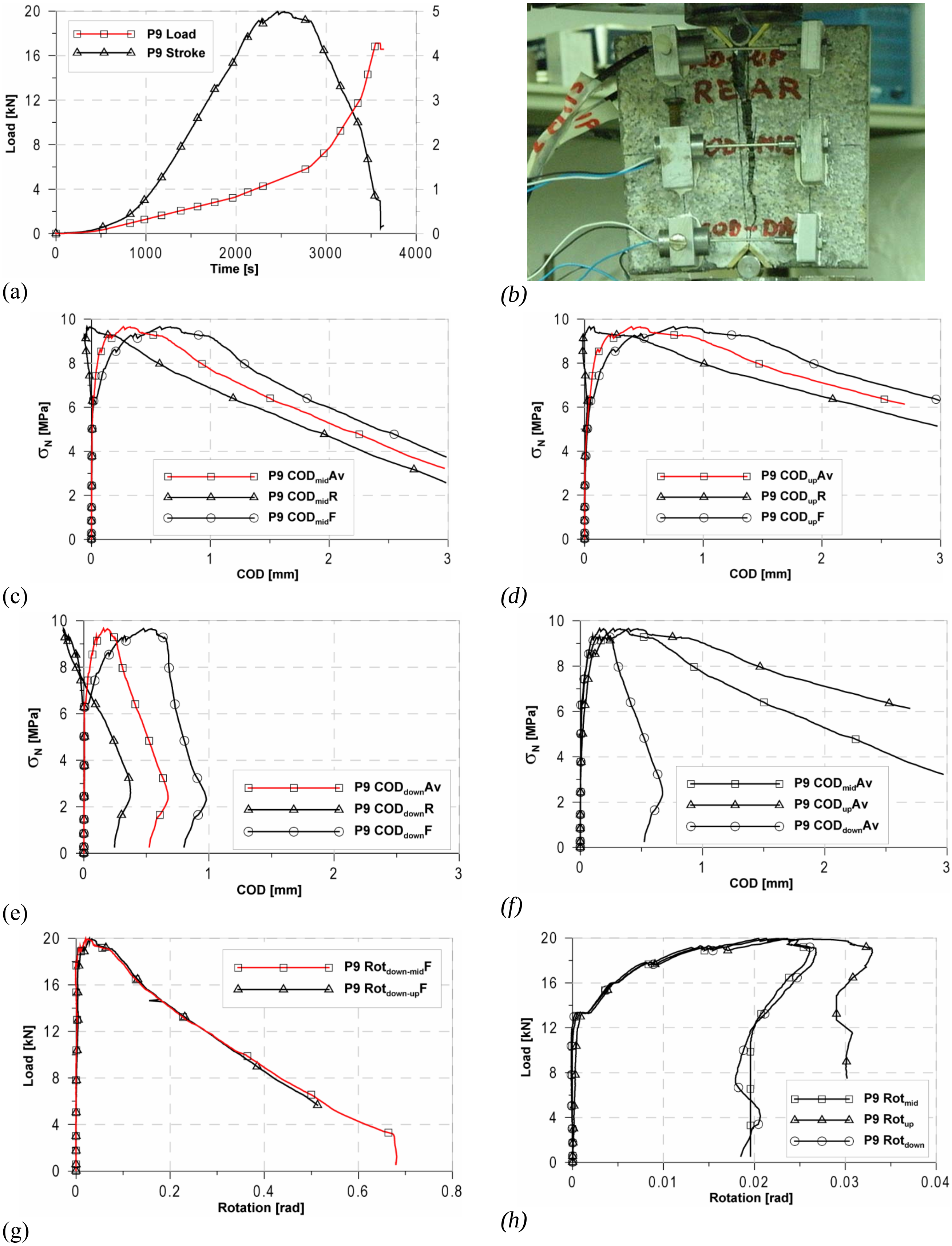


Figure 5. Specimen P9: (a,b) test parameter control and crack propagation; (c,d,e ) COD propagation in the mid, up and down transducer location in the front and rear side; (f) average COD values in the up, mid and down location; (g,h) rotation along two axes: the one at right angle with the tile average plane and the vertical axis of the average plane at up, mid and down location.

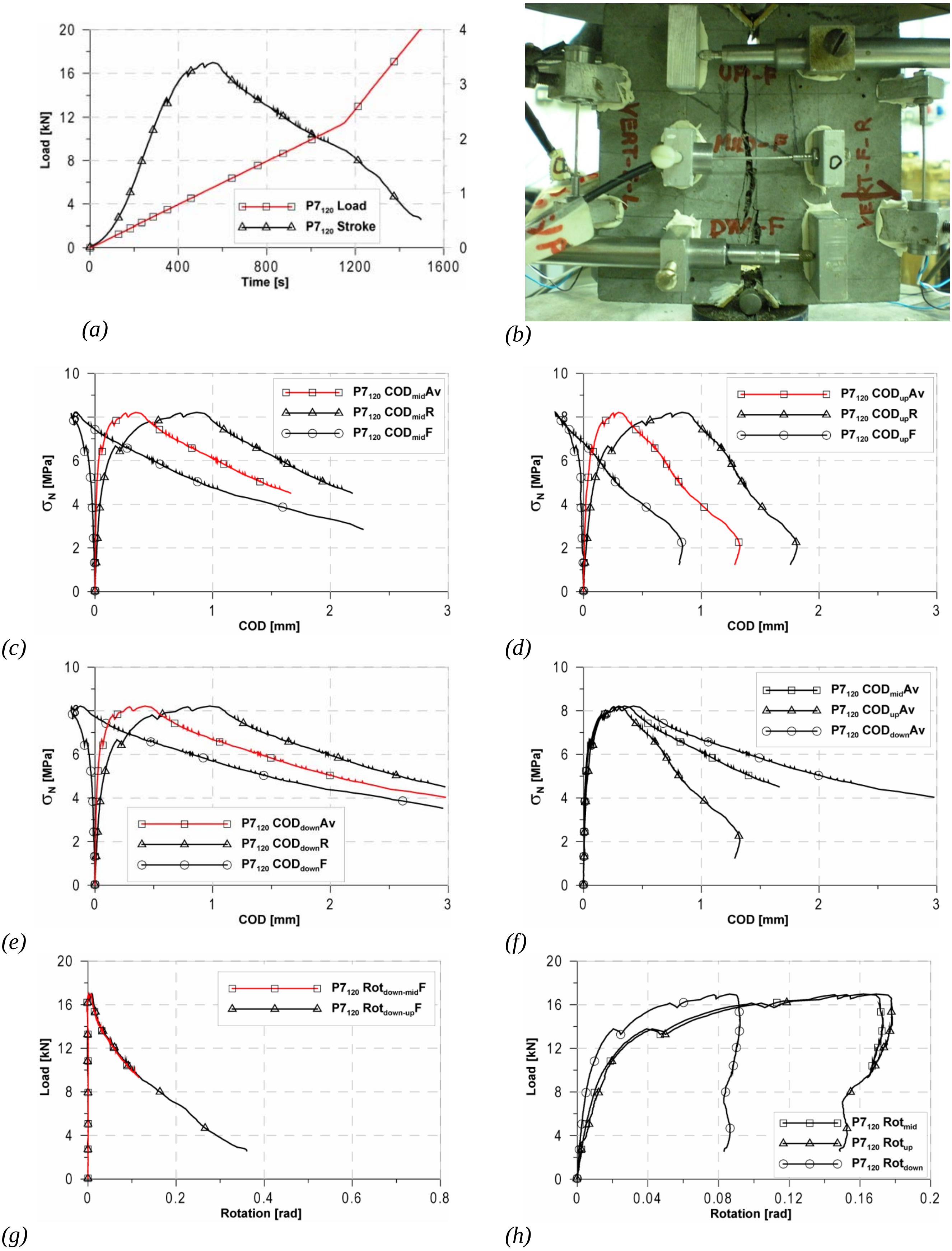


Figure 6. Specimen P7-120: (a,b) test parameter control and crack propagation; (c,d,e ) COD propagation in the mid, up and down transducer location in the front and rear side; (f) average COD values in the up, mid and down location; (g,h) rotation along two axes :the one at right angle with the tile average plane and the vertical axis of the average plane at up, mid and down location.

Due to the no friction assumption, the horizontal force is equal to the vertical component. The load vs. COD curve (Fig. 8a) is compared with the experimental curve corresponding to the test used to identify the post-peak energy dissipated adopted in the Hordjik's constitutive law ($P1_{120}$). The comparison highlights a very good trend, and a comparable peak load. A stiffer behaviour in proximity of the onset of first cracking can be caused by the linear behaviour selected in the pre-peak branch.

A nonlinear constitutive model in compression was introduced by means in a model proposed by Thorenfeldt (1987). The FE analysis was carried out by means of a plane stress non linear finite element method (NLFEA) with a total strain formulation.

A smeared-cracked approach was adopted, with a constant tension cut-off criterion that governs the initiation of cracks, and a full shear retention approach.

A fracture energy regularization was assumed and the tension stress-strain constitutive law was computed in DIANA with the value of crack band width, h, equal to $\sqrt{A}$ (A=element area).

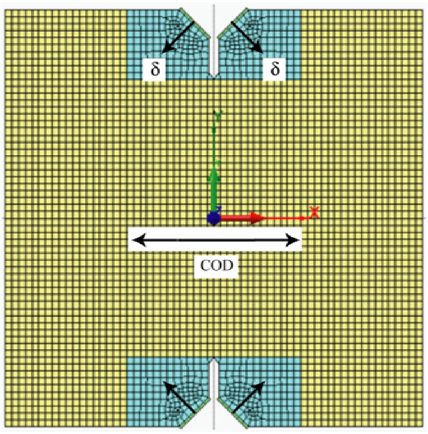


Figure 7. Adopted mesh for FE analysis (n. nodes: 11653; n. element: 3792; element type: CQ16M quadratic 8 nodes quadrilateral and CT12M quadratic 6 nodes plane stress).

First of all the results highlight very small total displacements in the cracked plane region and a quite constant stress along the critical depth at the peak load (Figs. 8b,c) and a quite rectangular mode I cracked region with a total width close to the half of the critical depth. The compressed arch is evident in Figure 8b,c with reference always to the peak load step. The tensile stress and crack opening displacement profiles along the critical depth are shown in Figure 9. These results show a not negligible meso-structure behavior which favors a post-peak load stability. This evidence clarifies that also in this simple test, the response does not correspond exactly to the constitutive law, although residual strength can be very well identified. Another very important result is connected with the lack of any significant shear component along the crack plane and this is essential to prevent spurious measures. The undamaged zones close to the outer vertical portions of the specimens could also tested in compression due to the small aggregate characterizing the material mix-design (2 mm) that 20x20x40 mm prisms can be regarded significant representative volumes.

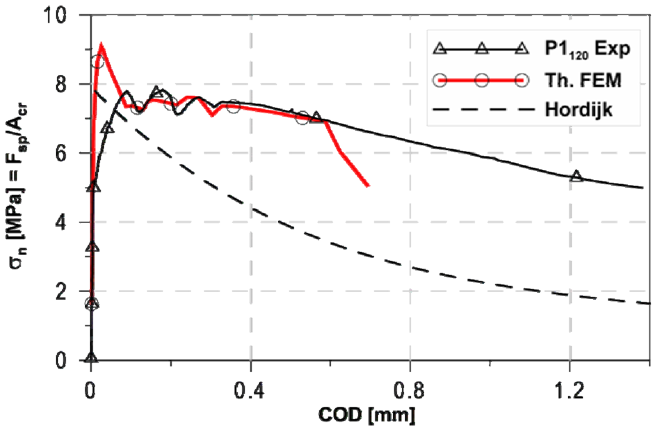


(a)

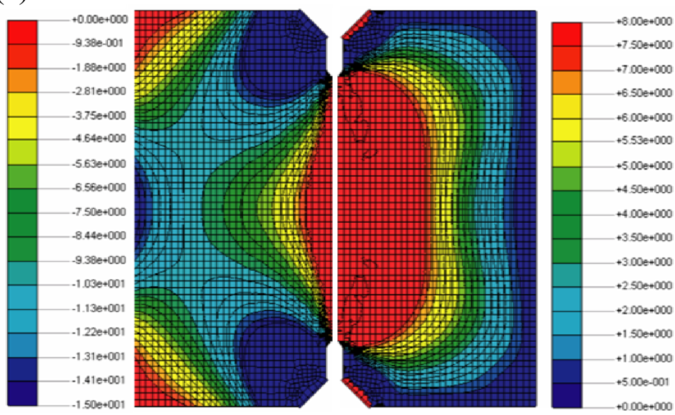

(b)

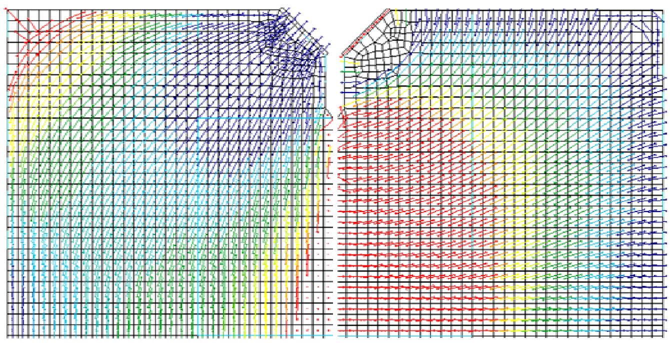

(c)

Figure 8. FE test results: (a) Theorical Vs experimental load-COD curve and tensile softening adopted law; (b,c) tensile and compressive principal stresses contour and vector representation at the peak load.

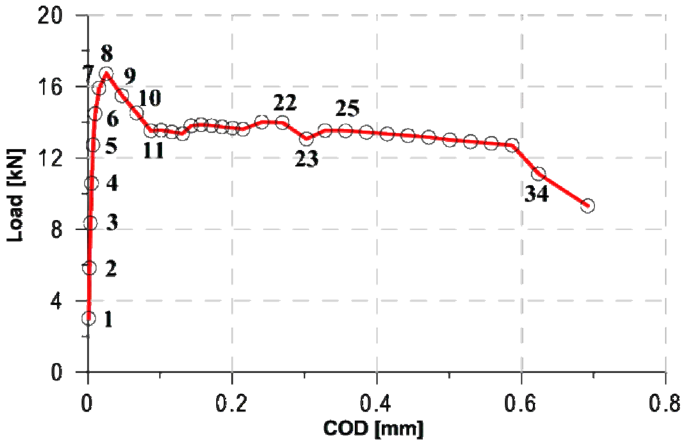


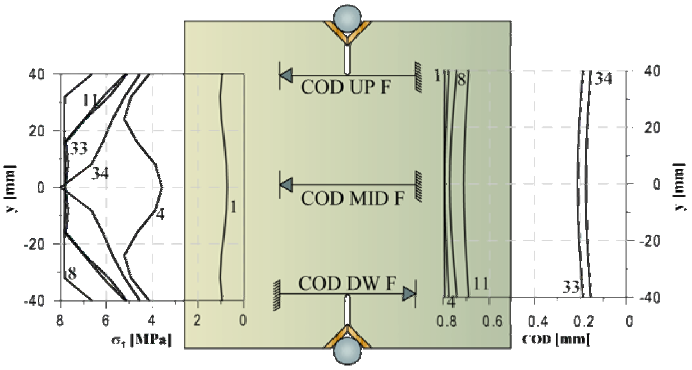


Figure 9. FE test results: uniaxial tensile stress and displacement profiles for elastic phase (step 1,4), peak load (step 8) and a final load step (step 11, 33, 34).

## 6 CONCLUDING REMARKS

On the basis of the preliminary experimental and numerical investigations carried out, the following remarks can be drawn.

Double Edge Wedge Splitting test here introduced is able to identify uniaxial tensile post-peak behavior for Fiber Reinforced Cementitious Composite by means of a uniaxial compression test.

The double compressed arches contributes to reduce the energy release associated to the unloaded regions and allows a quite regular test control by using stroke as feedback parameter.

A suitable instrument equipment allows the measure of two rotations around two axes: one at right angle with the tile average plane and around the vertical axis of the average plane: these rotation evolution are strictly related with fiber dispersion in the thickness and in the critical depth of the specimen.

By choosing different orientations of the notch axis, a multiaxial constitutive law identification can be performed: this possibility is very effective to assess the orthotropic behavior of casting flow-oriented fiber reinforced cementitious composites.

The specimen is relatively compact and light and the test can be easily carried out in every displacement controlled press.

The intuitive stress paths are confirmed by Finite Element investigation carried out following a smeared crack approach: a certain structure effect is highlighted by the difference between the constitutive law introduced for the material and the test response neglecting any effect of friction on the pushed zones. Further analyses could better clarify the relation between the material constitutive law and the test response.

The longer notch specimen (type B) prevents any compressive stress in the critical depth.

A pure mode I fracture takes place: in FE analyses no shear effects disturb the uniaxial tensile behavior.

FE analyses highlight two undamaged border regions in the specimen during the tests which are subjected only to small elastic compressive stresses and could be used to also identify uniaxial compressive behavior.

## 7 ACKNOWLEDGEMENTS


The research has been financially supported by INTERREG Project "Advanced Cementitious Composites In DEsign and coNstruction of safe Tunnel"- ACCIDENT -, ID 762-9770, Measure 2.2.


## REFERENCES


Bazant, Z.P. & Cedolin, L. 1983. Finite element modeling of crack band propagation, *ASCE Journal of Structural Engineering, 109(1):* pp. 69-92.

Brühwiler E. & Wittman F.H. 1990. The wedge splitting test, a new method of performing stable fracture mechanics tests. *Engineering Fracture Mechanics, 35* (1-3): 117-125.

Chen WF. and Yuan L. 1980. Tensile Strength of Concrete: Double-Punch Test. *Journal of the Structural Division,* 106 (8): 1673-1693.

di Prisco, M., Lamperti, M., Lapolla, S., Khurana, R.S. 2008. HPFRCC thin plates for precast roofing, *Proc. of Second Int. Symposium on Ultra High Performance Concrete, Kassel Germany*: 675-682.

di Prisco, M., Ferrara, L., Colombo, M., Mauri, M. 2004. On the identification of SFRC costitutive law in uniaxial tension – in Fiber reinforced concrete. di Prisco et al. (Eds.), *Proc. of 6th Rilem Symp. BEFIB 04, Varenna (Italy), PRO 39, Bagneaux Rilem Publications S.a.r.l.*. France. 827-836.

Ferrara, L., Ozyurt, N. and di Prisco, M. 2010. High mechanical performance of fiber reinforced cementitious composites: the role of "casting-flow induced" fiber orientation. Accepted by Materials and Structures.

Hordijk, D. 1991. Local approach to fatigue of concrete, Ph.D.Thesis, Delft University of Technology: pp. 207.

Thorenfeldt, E., Tomaszewicz, A., and Jensen, J. J. 1987. Mechanical properties of high-strength concrete and applications in design, *Proc. Symp. Utilization of High-Strength Concrete, Stavanger, Norway.*